Cone-beam computed tomography-guided endobronchial ultrasound using an ultrathin bronchoscope for diagnosis of peripheral pulmonary lesions: a prospective pilot study

Naoya Kawakita[1], Hiroaki Toba[1], Shinichi Sakamoto[1], Naoki Miyamoto[1], Mika Takashima[1], Yukikiyo Kawakami[1], Kazuya Kondo[2], Hiromitsu Takizawa[1]

[1]Department of Thoracic and Endocrine Surgery and Oncology, Institute of Biomedical Sciences, The University of Tokushima Graduate School, Tokushima, Japan; [2]Department of Oncological Medical Services, Graduate School of Biomedical Biosciences, Tokushima University, Tokushima, Japan

Contributions: (I) Conception and design: N Kawakita, H Toaba; (II) Administrative support: H Toba, H Takizawa, K Kondo; (III) Provision of study materials or patients: N Kawakita, S Sakamoto, N Miyamoto; (IV) Collection and assembly of data: S Sakamoto, N Miyamoto, M Takashima; (V) Data analysis and interpretation: N Kawakita, Y Kawakami; (VI) Manuscript writing: All authors; (VII) Final approval of manuscript: All authors.

Correspondence to: Naoya Kawakita, MD, PhD. Department of Thoracic and Endocrine Surgery and Oncology, Institute of Biomedical Sciences, The University of Tokushima Graduate School, 3-18-15, Kuramoto-cho, Tokushima 770-8503, Japan. Email: kawakita.naoya@tokushima-u.ac.jp.

Background: Multimodal transbronchial biopsy (TBB) may have improved diagnostic yield for peripheral pulmonary lesions suspected as lung cancer. Radial endobronchial ultrasound (R-EBUS) provides real-time imaging and confirmation of the location of the lesions. Cone-beam computed tomography (CBCT) can confirm that the forceps tip has reached the lesion before biopsy.

Methods: Patients with peripheral pulmonary lesions and a positive computed tomography (CT) bronchus sign (based on slice thickness of 1 mm) were prospectively enrolled. An ultrathin bronchoscope (UTB) and R-EBUS probe were advanced to the target bronchus. Thereafter, forceps were advanced, and CBCT was performed. R-EBUS was performed for re-navigation, if possible. The obtained EBUS and CBCT images were classified into "within" (type 1), "adjacent to" (type 2), or "far from" (type 3), based on the probe or forceps tip.

Results: For 20 lesions, the diagnostic yield was 85%. The primary EBUS images were of types 1, 2, and 3 in 12, 6, and 2 cases, respectively. The primary CBCT images were of types 1, 2, and 3 in 12, 6, and 2 cases, respectively. Primary EBUS and CBCT image types were equivalent in 14 cases. Of the 12 cases with type 1 primary EBUS image, 9 cases had a type 1 primary CBCT image, while 3 cases exhibited positional misalignment of the forceps tip. Re-navigation was required in 8 cases with types 2 and 3 primary CBCT images.

Conclusions: CBCT-guided TBB using an UTB and EBUS may enable real-time positioning guidance and better re-navigation in the diagnosis of peripheral pulmonary lesions.

Keywords: Cone-beam computed tomography (CBCT); endobronchial ultrasound (EBUS); transbronchial lung biopsy; ultrathin bronchoscope (UTB); virtual bronchoscopic navigation (VBN)

Introduction

The modality of bronchoscopic transbronchial biopsy (TBB) is developing rapidly. Its diagnostic yield is expected to further improve with the combined use of conventional and improved methods (1-4). An ultrathin bronchoscope (UTB) may also improve the diagnostic yield of TBB by enabling accessibility, bronchial selectivity, and maneuverability in peripheral small bronchi (5-10). However, the channel diameter of a UTB is as small as 1.2 mm; therefore, radial endobronchial ultrasound (R-EBUS) cannot be used for longer durations. Therefore, in order to reliably navigate a UTB and forceps to the lesions, virtual bronchoscopic navigation (VBN) and/or computed tomography (CT) have been used in combination with fluoroscopy (6,7,11,12). Recently, C-arm cone-beam CT (CBCT) systems, consisting of a C-arm gantry, X-ray tube, and flat-panel detector, have been introduced in the field of interventional radiology (13). CT-guided TBB using a UTB with a channel diameter of 1.2 mm has now been changed to CBCT-guided TBB using a UTB with a channel diameter of 1.2 mm (14). Previously, we compared CT-guided and CBCT-guided TBB using a UTB with a channel diameter of 1.2 mm using propensity score-matched analysis and showed that CBCT-guided TBB had a better diagnostic yield (15). The greatest merit of CBCT-guided TBB is that CBCT is taken with forceps inserted, which enables real-time biopsy.

In contrast, a bronchoscope with a channel diameter of 1.7 mm or more is required for R-EBUS. Additionally, a EBUS using a guide sheath (EBUS-GS) to improve bronchial selectivity is recommended, but the channel diameter should be 2 mm or more (16-19). Recently, a UTB with a channel diameter of 1.7 mm that can be used with R-EBUS has become available. Oki *et al.* (10,20) compared R-EBUS with this UTB, the so-called EBUS using an UTB (EBUS-UT) method, with R-EBUS using a conventional or thin bronchoscope through a randomized controlled trial and reported that EBUS-UT had a significantly better diagnostic yield. The EBUS-UT method is a very promising technique; however, because R-EBUS must be removed to allow biopsy, positional misalignment of the forceps tip may occur when inserting the biopsy forceps. Therefore, we hypothesized that the combined use of R-EBUS and CBCT using a UTB with a 1.7-mm channel diameter would facilitate bronchoscopy to reach the lesioned bronchus more reliably and enable real-time biopsy, thereby contributing to further improvement in diagnostic yield. The purpose of this study was to clarify the usefulness of TBB performed in combination with R-EBUS and CBCT using a UTB (CBCT-guided EBUS-UT) for the diagnosis of peripheral pulmonary lesions. We present the following article in accordance with the TREND reporting checklist (available at https://jtd.amegroups.com/article/view/10.21037/jtd-22-1369/rc).

Methods

Patients

Consecutive patients with undiagnosed peripheral pulmonary lesions who underwent CBCT-guided TBB using EBUS-UT were recruited at Tokushima University Hospital from January 2021 to October 2021 for this prospective pilot study. The inclusion criteria were as follows: (I) one or more peripheral pulmonary lesions suggestive of lung cancer; (II) lesions surrounded by normal lung parenchyma without any evidence of endobronchial abnormality on CT; and (III) a positive CT bronchus sign, either type A or B, according to Minezawa *et al.* (21). This study was conducted in accordance with the Declaration of Helsinki (as revised in 2013). The study was approved by the Tokushima University Hospital Institutional Review Board in February 2020 (No. 3672). Written informed consent was obtained from all patients for participation in this study.

Materials and procedural workflow

After local anesthesia with lidocaine and moderate sedation with intravenous midazolam, a UTB (BF-MP290F; Olympus Medical Systems, Tokyo, Japan: distal-end diameter, 3.0 mm and working channel diameter, 1.7 mm) was advanced to engage the target bronchus using VBN

Highlight box

Key findings
• The CBCT-guided EBUS-UT method showed a satisfactory diagnostic yield for detecting peripheral pulmonary lesions.

What is known and what is new?
• Re-navigation using CBCT can improve the accuracy of navigation and reliably engage the lesion using the tip of the EBUS probe and forceps tip.

What is the implication, and what should change now?
• CBCT-guided TBB using an UTB and EBSU may enable real-time positioning guidance and better re-navigation in the diagnosis of peripheral pulmonary lesions.
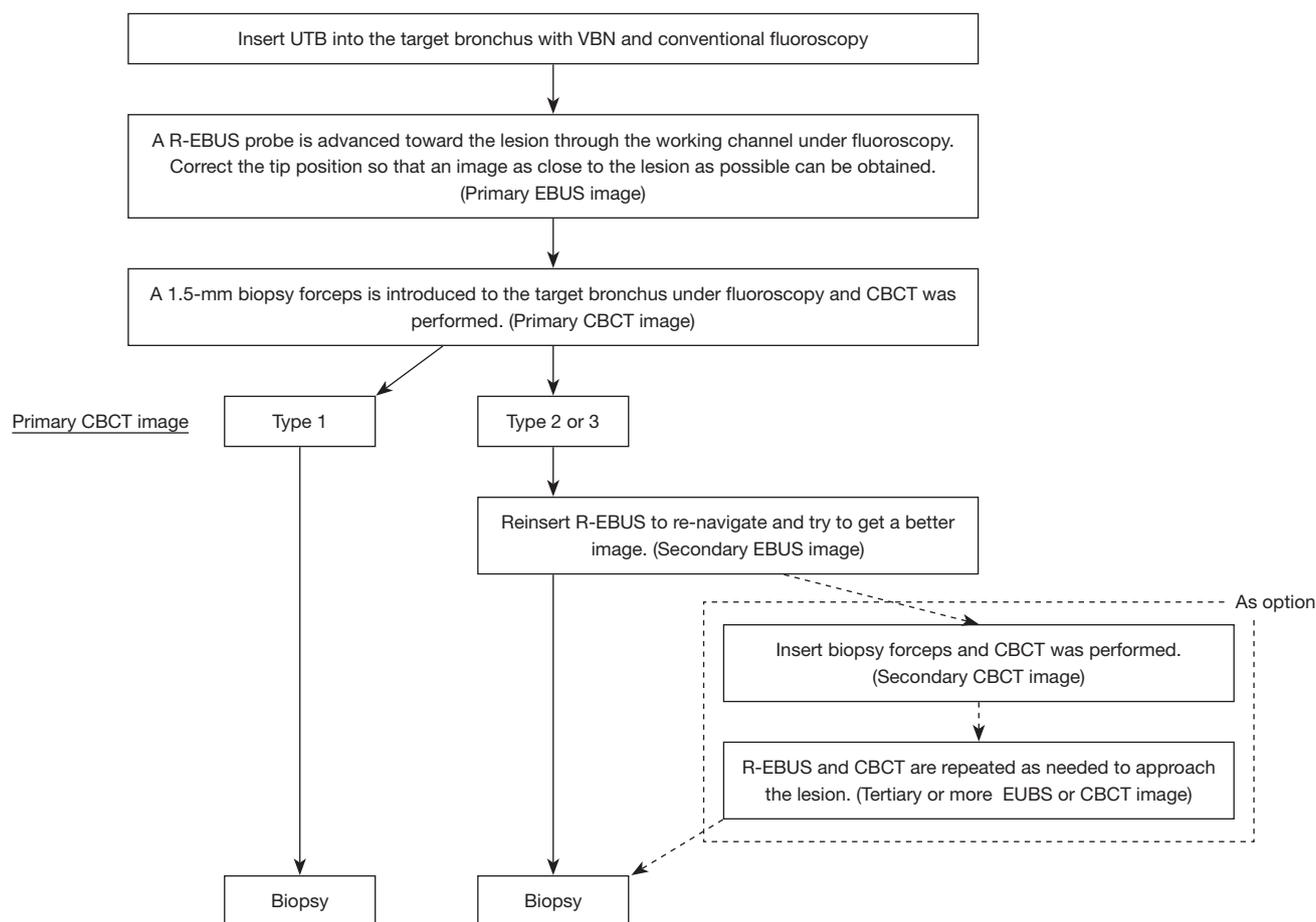

Figure 1 Procedural workflow of CBCT-guided EBUS for the diagnosis of peripheral pulmonary lesions using a UTB. UTB, ultrathin bronchoscope; VBN, virtual bronchoscopic navigation; R-EBUS, radial endobronchial ultrasound; CBCT, cone-beam computed tomography.

(SYNAPSE VINCENT; Fujifilm Medical, Tokyo, Japan) and conventional fluoroscopy (Artis Zeego, Siemens Healthcare, Forchheim, Germany). After reaching the target bronchus, a 1.4-mm R-EBUS probe (UM-S20-17S; Olympus Medical Systems) was advanced toward the lesion through the working channel under the guidance of conventional fluoroscopy. The obtained EBUS images were classified into three types based on the classification by Kurimoto *et al.* (17) (primary EBUS image). Type 1 EBUS images indicated "within", type 2 indicated "adjacent to", and type 3 indicated "invisible". The type with a smaller image number was considered a better EBUS and CBCT image (*Figures 1,2*). After the EBUS image was obtained, a 1.5-mm biopsy forceps (FB-433D; Olympus Medical Systems) was introduced through the working channel of the UTB directly into the target bronchus under the guidance of conventional fluoroscopy without augmented fluoroscopy.

After the biopsy forceps engaged the target bronchus, CBCT was performed during breath-holding using a 6-s acquisition protocol with 400 projection images acquired over a 200-degree rotation (Artis Zeego, Siemens Healthcare). Multi-planar reconstruction images were generated automatically on a dedicated workstation (Syngo X Workplace, Siemens Healthcare). Based on the relationship between the lesion and the forceps position, we classified the obtained images into three groups, as described in our previous report (primary CBCT image) (14). Type 1 CBCT image indicated that the forceps clearly reached the inside of the target lesion, type 2 indicated that the forceps reached adjacent to the lesion, and type 3 indicated that the forceps did not reach the lesion. Type 1 EBUS and CBCT, type 2 EBUS and CBCT, and type 3 EBUS and CBCT were recognized as equivalent images. If the primary CBCT image was type 1, a biopsy was performed. If it was type 2
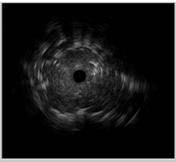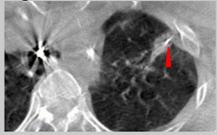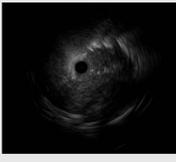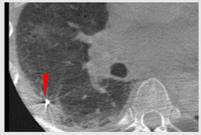
Image type	R-EBUS image		CBCT target forceps sign (CBCT image)
Type 1	Within		The forceps clearly reached the inside of the target lesion
Type 2	Adjacent to		The forceps have reached adjacent to the lesion (neither type 1 or 3)
Type 3	Invisible		The forceps could not reach the lesion
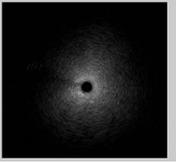
Figure 2 Classification of R-EBUS and CBCT image types. Red arrowheads show forceps tip. R-EBUS, radial endobronchial ultrasound; CBCT, cone-beam computed tomography.

or 3, the three-dimensional re-navigation toward the lesion was determined on the CBCT image and re-navigation was performed using R-EBUS. In the re-navigation procedure, first, based on the multi-planar reconstruction image obtained from the CBCT image, it was determined whether the target bronchus was ventral or dorsal and lateral or medial to the current forceps tip position. It was also determined if the position of the bronchoscope tip needed to be adjusted. Next, while viewing the two-dimensional fluoroscopic image of the front or side, the position and direction of the tip of the bronchoscope were adjusted, and the R-EBUS probe was advanced in the direction of the target bronchus. This EBUS image was defined as the secondary EBUS image. Thereafter, CBCT was performed if required and defined as the secondary CBCT image. Subsequently, tertiary or more EBUS or CBCT images were obtained and defined as required. The best image obtained during the examination (smaller numbers in each image type) was defined as the best EBUS/CBCT image. We obtained six biopsy samples and two brushing samples and performed bronchial alveolar lavage with 20 mL saline. If the tip of the forceps did not reach the lesion, only bronchial alveolar lavage with 20 mL saline was performed.

Diagnostic criteria

The diagnostic criteria used in the study have been described in our previous report (15). A diagnosis of malignancy was based on the presence of malignant-appearing cytology or histology. In the case of benign lesions, when bronchoscopy demonstrated a distinct histologic pattern (such as epithelioid granuloma, intra-alveolar organization, or cryptococcal organism) or the presence of bacteria accompanied by reasonable radiologic and clinical findings, we determined that the bronchoscopy was successful. However, if the forceps did not reach the lesion and no malignancy was found by histology or cytology, or if there was an inconclusive histologic diagnosis of non-specific fibrosis or inflammation, the patient was classified as "undiagnosed".

Statistical analysis

All continuous values were expressed as a mean (range).

Results

Twenty patients (14 male and 6 female) were enrolled in this study. Their mean age was 70.7 (range, 44–86) years, and the mean size of the lesion was 24.8 (range, 10–46) mm (*Table 1*). The CT appearances of the lesions were part-solid ground-glass opacity in 4 cases and completely solid in 16 cases. The CT bronchus sign, based on the classification by Minezawa *et al.* (21), was type A in 19 cases and type B in 1 case.

Table 1 Patients' characteristics of CBCT-guided EBUS-UT method (n=20)

Characteristics	N [%] or mean [range]
Age (years)	70.7 [44–86]
Gender	
Male	14 [70]
Female	6 [30]
Smoking history (pack-year)	28.3 [0–40]
SUVmax	7.4 [1.4–18.2]
Lesion location	
RU/RM/RL	6 [30]/2 [10]/6 [30]
LU/LL	4 [20]/2 [10]
Size of lesion (mm)	24.8 [10–46]
CT appearance	
Part solid GGO	4 [20]
Solid	16 [80]
CT bronchus sign	
Type A	19 [95]
Type B	1 [5]
Fluoroscopy	
Visible	11 [55]
Invisible	9 [45]

CBCT, cone-beam computed tomography; EBUS-UT, endobronchial ultrasound using an ultrathin bronchoscope; TBB, transbronchial biopsy; SUVmax, maximum standardized uptake value; RU, right upper lobe; RM, right middle lobe; RL, right lower lobe; LU, left upper lobe; LL, left lower lobe; CT, computed tomography; GGO, ground grass opacity.

Table 2 Diagnostic yields and outcome of TBB using CBCT-guided EBUS-UT method

Diagnostic yields/outcomes	Yields % [n/N] or mean [range]
Diagnostic yields	
Overall	85.0 (17/20)
Final diagnosis	
Malignant lesion	93.8 (15/16)
Benign lesion	50.0 (2/4)
Fluoroscopy	
Visible	90.8 (10/11)
Invisible	77.8 (7/9)
Primary EBUS image	
Type 1	83.3 (10/12)
Type 2	100.0 (6/6)
Type 3	50.0 (1/2)
Primary CBCT image	
Type 1	91.7 (11/12)
Type 2	100.0 (6/6)
Type 3	0.0 (0/2)
Best EBUS image	
Type 1	81.3 (13/16)
Type 2	100.0 (4/4)
Best CBCT image	
Type 1	93.8 (15/16)
Type 2	66.7 (2/3)
Type 3	0.0 (0/1)
Outcome	
Complications	
Pneumothorax	5.0 (1/20)
Mean number of CBCT scan	1.3 [1–3]
Mean examination time (min)	44 [32–93]

TBB, transbronchial biopsy; CBCT, cone-beam computed tomography; EBUS-UT, endobronchial ultrasound using an ultrathin bronchoscope; EBUS, endobronchial ultrasound.

Eleven lesions (55%) were fluoroscopically visible (*Table 1*). The overall diagnostic yield was 85% (17/20), and the diagnostic yield for malignant lesions was 93.8% (*Table 2*). The diagnostic yields of the primary EBUS image for types 1, 2, and 3 were 83.3% (10/12), 100% (6/6), and 50% (1/2), respectively, and those of the primary CBCT image for types 1, 2, and 3 were 91.7% (11/12), 100% (6/6), and 0% (0/2), respectively. The mean number of CBCT scans was 1.3 (range, 1–3). As a complication, pneumothorax was observed in 1 case (5%); it resolved after chest tube drainage. The mean examination time was 44 (range, 32–93) min. The details of the examination and EBUS/CBCT image types are shown in *Figure 3*. The primary EBUS images were of type 1 in 12 cases, of which the primary CBCT image was of type 1 in 9 cases, and the remaining 3 cases exhibited positional misalignment of the forceps tip. Therefore, re-navigation was performed in these 3 cases using R-EBUS.
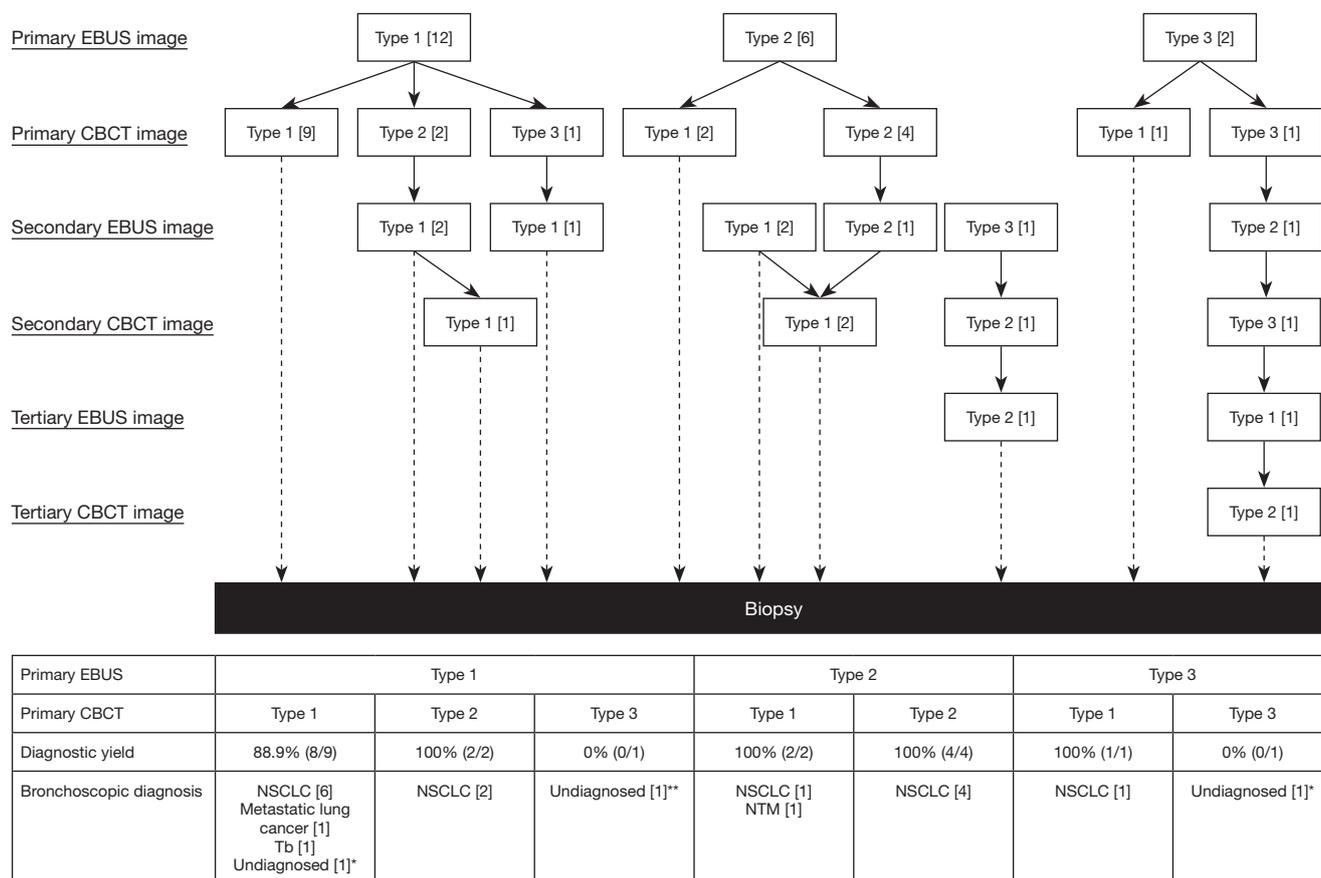
Primary EBUS image — Type 1 [12]   Type 2 [6]   Type 3 [2]

Primary CBCT image — Type 1 [9]   Type 2 [2]   Type 3 [1]   Type 1 [2]   Type 2 [4]   Type 1 [1]   Type 3 [1]

Secondary EBUS image — Type 1 [2]   Type 1 [1]   Type 1 [2]   Type 2 [1]   Type 3 [1]   Type 2 [1]

Secondary CBCT image — Type 1 [1]   Type 1 [2]   Type 2 [1]   Type 3 [1]

Tertiary EBUS image — Type 2 [1]   Type 1 [1]

Tertiary CBCT image — Type 2 [1]

Biopsy

Primary EBUS	Type 1			Type 2		Type 3	
Primary CBCT	Type 1	Type 2	Type 3	Type 1	Type 2	Type 1	Type 3
Diagnostic yield	88.9% (8/9)	100% (2/2)	0% (0/1)	100% (2/2)	100% (4/4)	100% (1/1)	0% (0/1)
Bronchoscopic diagnosis	NSCLC [6] Metastatic lung cancer [1] Tb [1] Undiagnosed [1]*	NSCLC [2]	Undiagnosed [1]**	NSCLC [1] NTM [1]	NSCLC [4]	NSCLC [1]	Undiagnosed [1]*

Figure 3 Details of the image type and flow of investigations to biopsy. *, diagnosed with non-specific inflammation after surgical biopsy; **, diagnosed with lymphoma after surgical biopsy. EBUS, endobronchial ultrasound; CBCT, cone-beam computed tomography; NSCLC, non-small cell lung cancer; Tb, mycobacterium tuberculosis infection; NTM, non-tuberculosis mycobacteria infection.

The primary EBUS images were of type 2 in 6 cases, of which the primary CBCT image was of type 1 in 2 cases; therefore, biopsy was performed in these 2 cases. In the remaining 4 cases, the primary CBCT images were of type 2; therefore, biopsy was performed after re-navigation. As a result, the diagnostic yield of the primary EBUS image type 2 was 100% in the 6 cases. Of the total 20 cases, re-navigation was performed in 8 cases of primary CBCT image types 2 and 3. Type 1 primary EBUS images were observed in 12 cases (60%), but the best type 1 EBUS images, including images after re-navigation, were observed in 16 cases (80%; *Table 2*). *Figure 4* shows the typical EBUS and CBCT image types and their correction processes.

Discussion

In this study, we introduced the CBCT-guided EBUS-UT method, which showed a good diagnostic yield of 85%, and clarified consistency in EBUS/CBCT image types. The diagnostic yield can be increased to almost 70–80% by single or multimodal TBB using VBN, electromagnetic navigation bronchoscopy, R-EBUS, GS, CT (CBCT), and a UTB (1,2). For TBB using R-EBUS, EBUS-UT has demonstrated the highest diagnostic yield in prospective studies (10,20). We also showed through a previous retrospective study that TBB with a UTB may have a higher diagnostic yield when guided by CBCT compared to that with CT (15). Therefore, we combined CBCT with EBUS-UT and found that the diagnostic yield was 85% and sensitivity for malignancy was 93.8%. These are comparable to the corresponding parameters of conventional multimodal TBB.

In this study, we verified consistency between the primary EBUS image type obtained by inserting the R-EBUS
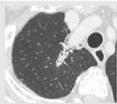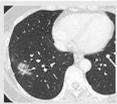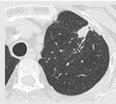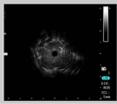
Image type and its process	Case 1	Case 2	Case 3	Case 4
	EBUS type 1 → CBCT type 1	EBUS type 1 → CBCT type 2 → EBUS type 1 → CBCT type 1	EBUS type 2 → CBCT type 1	EBUS type 2 → CBCT type 2 → EBUS type 1 → CBCT type 1
Thin slice CT				
Primary EBUS				
Primary CBCT				
Secondary EBUS				
Secondary CBCT				
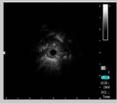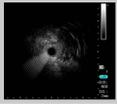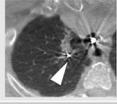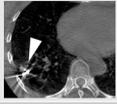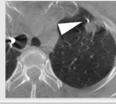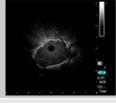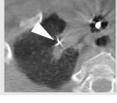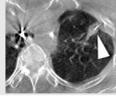
Figure 4 Typical EBUS and CBCT image types with their correction processes. White arrowheads indicate the forceps tip. EBUS, endobronchial ultrasound; CBCT, cone-beam computed tomography; CT, computed tomography.

probe and CBCT image type obtained by inserting forceps, which is a novel technique. In 14 of 20 cases, the primary EBUS and primary CBCT image types were equivalent. In particular, 12 cases exhibited type 1 primary EBUS images, of which 9 cases (75%) exhibited type 1 primary CBCT images. In the remaining 3 cases (25%), the R-EBUS probe and forceps may have been inserted into different bronchi. This may be due to the fact that the forceps may take a different trajectory compared to that of the R-EBUS probe when the thin flexible scope is significantly flexed/retroflexed. As a result, it may have been the reason for the plateaued diagnostic yield at approximately 80%, even when type 1 (within) was obtained by R-EBUS (17,22-25). It should be noted that there was a 100% diagnostic yield in 6 cases with type 2 primary EBUS images (adjacent to) in this study. As shown in past reports, type 2 EBUS images have a lower diagnostic yield than type 1 EBUS images, with a diagnostic yield of approximately 50% (17,22-25). According to the results of this study, 2 of the 6 cases with type 2 primary EBUS images subsequently showed type 1 primary CBCT images and underwent biopsy. The remaining 4 cases with type 2 primary EBUS images subsequently showed type 2 primary CBCT images. These 4 cases underwent re-navigation using R-EBUS based on

the primary CBCT image (*Figure 3*). When the R-EBUS probe and the forceps tip are in proximity to the lesion, the CBCT image can help in determining whether re-navigation is possible and the direction of three-dimensional correction (14).

Further, 1 case with a type 3 primary EBUS image had a type 1 primary CBCT image. In this case, the bronchioles were obstructed by the tumor and could not be visualized using ultrasound; however, it is probable that CBCT determined that the tip of the forceps had reached the center of the tumor. In fact, a type 1 EBUS image was obtained after several biopsies. CBCT may also be useful for confirming access to bronchioles obstructed by a tumor.

The combined use of R-EBUS and CBCT has been previously reported, and its diagnostic yield is 70–75.1% (26-29). Although the procedural workflow employed in these studies was slightly different from that in ours, all these reports involved the use of conventional or thin bronchoscopes with an outer diameter of ≥4 mm. To the best of our knowledge, this is the first study performed using a UTB. As a result, the diagnosis rate in our study was 85%, which is satisfactory for early pilot studies. Verhoeven *et al.* (27) reported that the combined use of R-EBUS and CBCT had a higher navigation success rate than the EMN

approach. Yu *et al.* (29) compared the diagnostic yield of TBB and R-EBUS separately with the combination of R-EBUS and CBCT and reported that the latter had a higher diagnostic yield. Casal *et al.* (26) reported that re-navigation using CBCT can increase the success rate of navigation and diagnostic yield. These findings showed that CBCT is a reliable modality for navigation, and re-navigation using CBCT can increase the reliability of engaging target lesions. Our results showed that type 1 primary EBUS images were observed in 12 cases (60%), but the best type 1 EBUS image including the image after re-navigation increased to 16 cases (80%). Oki *et al.* (20) compared the diagnostic yield of TBB with EBUS-UT and EBUS-GS and reported that the former had a higher diagnostic yield. This could be because the ultrasound probe could be introduced into the lesion more frequently in the EBUS-UT group than in the EBUS-GS group. Therefore, they concluded that the EBUS-UT method should be used to introduce the biopsy instrument accurately in the leading bronchus. Therefore, using the CBCT-guided EBUS-UT method described in this study, in addition to confirming the engagement of the lesion by the ultrasound probe using EBUS, the engagement of the lesion by the forceps tip can be determined using CBCT. Furthermore, by exploring the possibility of re-navigation using CBCT, lesion engagement could be more predictable.

Radiation exposure could not be evaluated in this study. Previous CBCT-guided TBB studies have reported radiation doses of 4.3–23 mSv (26,30,31). Radiation exposure has been shown to decrease with increasing experience (31). According to our past reports, the mean number of CBCT images obtained using CBCT-guided TBB that employed a UTB with a small channel diameter was 1.8 (range, 1–5), which decreased to 1.3 (range, 1–3) (14,15). This could be due to the combined use of R-EBUS and CBCT, in addition to increased experience. The CBCT-guided EBUS-UT method can reduce radiation exposure to a greater extent than the former CBCT-guided TBB using a UTB.

The limitations of this study should be considered. First, as we included a limited number of cases, this could be considered a pilot study without any control group. Therefore, superiority over CBCT-guided TBB using a UTB with a small channel diameter or EBUS-UT TBB could not be demonstrated. Satisfactory results were obtained from this study, and prospective or retrospective comparative studies with more cases should be performed. Second, since this was a pilot study, the target lesions were slightly large tumors with the mean size of the lesion 24.8

(range, 10–46) mm with a positive CT bronchus sign; the majority, 16 of 20 (80%), were solid lesions. Since these were considered to be target lesions with a good diagnosis yield, additional case accumulation is required to further evaluate diagnostic yield. Third, the procedural workflow in this study did not exclude patients who did not require CBCT. Of the 12 cases with type 1 primary EBUS images, 3 cases with type 2 primary CBCT images required re-navigation based on the primary CBCT images. In 9 cases with type 1 primary EBUS images and type 1 primary CBCT images, it was possible that primary CBCT imaging could have been omitted. As mentioned above, by using an R-EBUS combination with CBCT-guided TBB using a UTB, there is a possibility that the number of CBCT images can be reduced. For further radiation exposure reduction, it would be necessary to analyze cases in which primary EBUS and CBCT images do not match. Thereby, in the future, patients' exposure to radiation can be further reduced by identifying those in whom primary CBCT imaging is not essential. Also, in patients for whom CBCT can be omitted, it is expected that the current mean examination time of 44 minutes will be further shortened.

Conclusions

In this pilot study, the CBCT-guided EBUS-UT method showed a satisfactory diagnostic yield for detecting peripheral pulmonary lesions. Re-navigation using CBCT can improve the accuracy of navigation and reliably engage the lesion using the tip of the EBUS probe and forceps tip.

Footnote

Reporting Checklist: The authors have completed the TREND reporting checklist. Available at https://jtd.amegroups.com/article/view/10.21037/jtd-22-1369/rc

Data Sharing Statement: Available at https://jtd.amegroups.com/article/view/10.21037/jtd-22-1369/dss

Peer Review File: Available at https://jtd.amegroups.com/article/view/10.21037/jtd-22-1369/prf

Conflicts of Interest: All authors have completed the ICMJE

uniform disclosure form (available at https://jtd.amegroups.com/article/view/10.21037/jtd-22-1369/coif). H Takizawa serves as an unpaid editorial board member of *Journal of Thoracic Disease*. The other authors have no conflicts of interest to declare.

Ethical Statement: The authors are accountable for all aspects of the work in ensuring that questions related to the accuracy or integrity of any part of the work are appropriately investigated and resolved. This study was conducted in accordance with the Declaration of Helsinki (as revised in 2013). The study was approved by the Tokushima University Hospital Institutional Review Board in 2020 (No. 3622), and informed consent was obtained from all individual participants.

References

1. Wang Memoli JS, Nietert PJ, Silvestri GA. Meta-analysis of guided bronchoscopy for the evaluation of the pulmonary nodule. Chest 2012;142:385-93.
2. Ishiwata T, Gregor A, Inage T, et al. Advances in interventional diagnostic bronchoscopy for peripheral pulmonary lesions. Expert Rev Respir Med 2019;13:885-97.
3. Shen YC, Chen CH, Tu CY. Advances in Diagnostic Bronchoscopy. Diagnostics (Basel) 2021;11:1984.
4. Gasparini S, Mei F, Bonifazi M, et al. Bronchoscopic diagnosis of peripheral lung lesions. Curr Opin Pulm Med 2022;28:31-6.
5. Kobayashi T, Shimamura K, Hanai K, et al. Computed tomography-guided bronchoscopy with an ultrathin fiberscope. Diagn Ther Endosc 1996;2:229-32.
6. Shinagawa N, Yamazaki K, Onodera Y, et al. CT-guided transbronchial biopsy using an ultrathin bronchoscope with virtual bronchoscopic navigation. Chest 2004;125:1138-43.
7. Matsuno Y, Asano F, Shindoh J, et al. CT-guided ultrathin bronchoscopy: bioptic approach and factors in predicting diagnosis. Intern Med 2011;50:2143-8.
8. Asano F. Advanced bronchoscopy for the diagnosis of peripheral pulmonary lesions. Respir Investig 2016;54:224-9.
9. Ishiwata T, Gregor A, Inage T, et al. Bronchoscopic navigation and tissue diagnosis. Gen Thorac Cardiovasc Surg 2020;68:672-8.
10. Oki M, Saka H, Asano F, et al. Use of an Ultrathin vs Thin Bronchoscope for Peripheral Pulmonary Lesions: A Randomized Trial. Chest 2019;156:954-64.
11. Tsushima K, Sone S, Hanaoka T, et al. Comparison of bronchoscopic diagnosis for peripheral pulmonary nodule under fluoroscopic guidance with CT guidance. Respir Med 2006;100:737-45.
12. Shinagawa N, Yamazaki K, Onodera Y, et al. Factors related to diagnostic sensitivity using an ultrathin bronchoscope under CT guidance. Chest 2007;131:549-53.
13. Kalender WA, Kyriakou Y. Flat-detector computed tomography (FD-CT). Eur Radiol 2007;17:2767-79.
14. Ali EAA, Takizawa H, Kawakita N, et al. Transbronchial Biopsy Using an Ultrathin Bronchoscope Guided by Cone-Beam Computed Tomography and Virtual Bronchoscopic Navigation in the Diagnosis of Pulmonary Nodules. Respiration 2019;98:321-8.
15. Kawakita N, Takizawa H, Toba H, et al. Cone-beam computed tomography versus computed tomography-guided ultrathin bronchoscopic diagnosis for peripheral pulmonary lesions: A propensity score-matched analysis. Respirology 2021;26:477-84.
16. Kikuchi E, Yamazaki K, Sukoh N, et al. Endobronchial ultrasonography with guide-sheath for peripheral pulmonary lesions. Eur Respir J 2004;24:533-7.
17. Kurimoto N, Miyazawa T, Okimasa S, et al. Endobronchial ultrasonography using a guide sheath increases the ability to diagnose peripheral pulmonary lesions endoscopically. Chest 2004;126:959-65.
18. Asahina H, Yamazaki K, Onodera Y, et al. Transbronchial biopsy using endobronchial ultrasonography with a guide sheath and virtual bronchoscopic navigation. Chest 2005;128:1761-5.
19. Yoshikawa M, Sukoh N, Yamazaki K, et al. Diagnostic value of endobronchial ultrasonography with a guide sheath for peripheral pulmonary lesions without X-ray fluoroscopy. Chest 2007;131:1788-93.
20. Oki M, Saka H, Ando M, et al. Ultrathin Bronchoscopy with Multimodal Devices for Peripheral Pulmonary Lesions. A Randomized Trial. Am J Respir Crit Care Med 2015;192:468-76.
21. Minezawa T, Okamura T, Yatsuya H, et al. Bronchus

sign on thin-section computed tomography is a powerful predictive factor for successful transbronchial biopsy using endobronchial ultrasound with a guide sheath for small peripheral lung lesions: a retrospective observational study. BMC Med Imaging 2015;15:21.

22. Okachi S, Imai N, Imaizumi K, et al. Factors Affecting the Diagnostic Yield of Transbronchial Biopsy Using Endobronchial Ultrasonography with a Guide Sheath in Peripheral Lung Cancer. Intern Med 2016;55:1705-12.

23. Ali MS, Trick W, Mba BI, et al. Radial endobronchial ultrasound for the diagnosis of peripheral pulmonary lesions: A systematic review and meta-analysis. Respirology 2017;22:443-53.

24. Bae S, Lim S, Ahn JJ, et al. Diagnosing peripheral lung lesions using endobronchial ultrasonography with guide sheath: A prospective registry study to assess the effect of virtual bronchoscopic navigation using a computed tomography workstation. Medicine (Baltimore) 2020;99:e19870.

25. Park S, Yoon HY, Han Y, et al. Diagnostic yield of additional conventional transbronchial lung biopsy following radial endobronchial ultrasound lung biopsy for peripheral pulmonary lesions. Thorac Cancer 2020;11:1639-46.

26. Casal RF, Sarkiss M, Jones AK, et al. Cone beam computed tomography-guided thin/ultrathin bronchoscopy for

diagnosis of peripheral lung nodules: a prospective pilot study. J Thorac Dis 2018;10:6950-9.

27. Verhoeven RLJ, Fütterer JJ, Hoefsloot W, et al. Cone-Beam CT Image Guidance With and Without Electromagnetic Navigation Bronchoscopy for Biopsy of Peripheral Pulmonary Lesions. J Bronchology Interv Pulmonol 2021;28:60-9.

28. Verhoeven RLJ, Vos S, van der Heijden EHFM. Multi-modal tissue sampling in cone beam CT guided navigation bronchoscopy: comparative accuracy of different sampling tools and rapid on-site evaluation of cytopathology. J Thorac Dis 2021;13:4396-406.

29. Yu KL, Yang SM, Ko HJ, et al. Efficacy and Safety of Cone-Beam Computed Tomography-Derived Augmented Fluoroscopy Combined with Endobronchial Ultrasound in Peripheral Pulmonary Lesions. Respiration 2021;100:538-46.

30. Bowling MR, Brown C, Anciano CJ. Feasibility and Safety of the Transbronchial Access Tool for Peripheral Pulmonary Nodule and Mass. Ann Thorac Surg 2017;104:443-9.

31. Verhoeven RLJ, van der Sterren W, Kong W, et al. Cone-beam CT and Augmented Fluoroscopy-guided Navigation Bronchoscopy: Radiation Exposure and Diagnostic Accuracy Learning Curves. J Bronchology Interv Pulmonol 2021;28:262-71.